行政院國家科學委員會補助專題研究計畫成果報告

※※※※※※※※※※※※※※※※※※※※※※※※※
※　　　　　　　　　　　　　　　　　　　　　　　　※
※　多張透視投影影像間強健式點特徵抽取與快速特徵比對技術　※
※　　　　　　　　　　　　　　　　　　　　　　　　※
※　　　　　　　　　　　　　　　　　　　　　　　　※
※　　　　　　　　　　　　　　　　　　　　　　　　※
※※※※※※※※※※※※※※※※※※※※※※※※※

計畫類別：■個別型計畫　　□整合型計畫

計畫編號：

執行期間： 95 年 8 月 1 日至 97 年 7 月 31

計畫主持人：陳　稔教授

本成果報告包括以下應繳交之附件：

□赴國外出差或研習心得報告一份

□赴大陸地區出差或研習心得報告一份

□出席國際學術會議心得報告及發表之論文各一份

□國際合作研究計畫國外研究報告書一份

執行單位：交通大學資訊工程學系

中　華　民　國 九十六 年 五 月 三十日

多張透視投影影像間強健式點特徵抽取與快速特徵比對技術

Robust Point Feature Point Extraction and High-Efficiency Point Matching for Multiple Perspective View Registering

計畫編號：95-2221-E-009-216-MY2

執行期限：95 年 8 月 1 日至 97 年 7 月 31 日

主持人：陳稔教授 / 國立交通大學資工系

E-mail: zchen@csie.nctu.edu.tw Tel: 03-5731875

1. Introduction

In computer vision various applications related to object pose determination, motion tracking, camera parameter estimation, object recognition and perspective reconstruction we need feature points with discriminating power to perform these tasks, no matter whether we use stereo views, multiple views or a view sequence. Also, we need to find the point correspondences across the views. Due to noise and occlusion and other reasons not all the feature points extracted are commonly visible across the different views, so the point correspondence finding is not an easy task. The conventional point matching method is based on image correlation, plus the use of ordering constraint and eipolar constraint to aid the matching. A dynamic programming [36] is applied to speed up the point matching search. However, when the camera viewpoints change widely, the above method becomes not suitable.

In the previous NSC research project we have developed the Gabor-filtering technique using the multi-scale and multi-orientation concepts to find the robust feature points. These feature points reflect the local pattern structure information to facilitating the point matching. The fundamental problem of point matching for image registration is to recover the 2D spatial transformation between two images taken under different viewing specifications. There are various image registration methods in the literature.

Different methods [1]-[13] were proposed to meet different requirements. However, there is still a need to find the optimal solution under the more desirable conditions. In the following we shall consider four general issues simultaneously in the view registration problem:

(1) The generality of spatial transformation: The spatial transformation between two images is often approximated by an affine transformation or a similarity transformation [12, 13]. However, both of them are special cases of a

homography (2D projective matrix). The homography deals with the projective distortion problem in addition to the effects of rotation, translation and scaling.

(2) View registration time complexity: There are two classes of image registration algorithms in estimating a particular 2D spatial transformation depending on whether an initial point matching is executed. In the first class of algorithms with an initial point matching, the time complexity for the initial matching is of the order $O(nm)$, where n and m are the total numbers of feature points in the reference and sensed images, respectively. Then the estimation of the underlying spatial transformation will be performed using the matching point pairs found[14-25]. On the other hand, the second class of algorithms does not perform the initial point matching. Instead, they first select a subset of points to compute the transformation matrix and then verify if the remaining points in the two point sets confirm the estimated transformation matrix. The time complexity of this kind of approaches ranges from $O(n^3 m^3)$ to $O(n^4 m^4)$, depending on the total number of feature points n and m used in the two views.

(3) Noise sensitivity: In real applications, images are spoiled by noise. The window-based approaches are more suitable than the pixel-based approaches to counteract the noise effect. Only the robust feature points should be used in the presence of the noise.

(4) Occlusion or partial matching: If the scenes in the two images to be registered are partially overlapped, the global registration methods such as the moment-based [32] and Fourier-based [33, 34] methods are inappropriate. The registration method based on the local information is more suitable. Moreover, the detection of the overlapping area of the two images is important to the registration problem.

The main ideas of our approach are described below.

(1) Robust feature point extraction under a more general view transformation: To find the robust feature points under a more general view transformation such as homography, we use the multi-scale and multi-orientation Gabor-based feature points developed in the previous NSC project. These feature points turn out to be virtually invariant under the homorgraphy transformation considered.

(2) View registration time complexity under the affine and homography transformations: For computational efficiency, we first approximate the homography as an affine and solve for an

approximate solution. Then we use an iterative algorithm to refine the solution subject to the homography transformation if the approximate solution representation a good initial solution. The computational complexity of our affine transformation estimation can be reduced based on the properties of the Gabor-based feature points. Moreover, to avoid a blind point matching among the all possible candidates, we shall plan the matching order in an off-line fashion based on the reference image information beforehand. With these planning strategies, promising point pairs can be found to lead to a good solution as quickly as possible.

(3) Occlusion handling or partial matching: To avoid blindly selecting feature points from a region where part of the object scene is not visible in the sensed image, we partition the reference image into four sub-regions in advance. Later, we apply an on-line mechanism to detect the potential occluded regions in the reference image to avoid selecting the matching point pairs from these regions.

(4) Noise insensitivity: The Gabor-based feature points with large energy and stable orientation prove to be less likely to be corrupted by noise. Therefore, the energy and principal orientation factors of the Gabor-based feature points can be taken into account in the selection of the candidate feature points.

The rest of the paper is organized as follows. In section 2, we introduce our invariant feature point extraction and the vector representation of the feature points under the similarity transformation. Next, we discuss how the affine transformation can be determined by using only two Gabor-based feature points along with their principal orientations to reduce the combinational complexity. In Section 3, we refine the approximate solution under a homography transformation by applying an iterative process, called ICPM. Section 5 gives our overall registration algorithm including the off-line planning strategies and the on-line registration steps. The experimental results are reported in Section 6.

2. The Gabor-based feature point

In our previous work [35], we apply a multi-scale and multi-orientation Gabor filtering technique to obtain a set of energy maps of a given image and then manage to get a single ‘maximum energy map’ by retaining the maximum energy at the principal scale (s_d) for each image point. We extract a set of Gabor-based feature points from the maximum energy map.

We use a feature vector

$\vec{V}_{p_i}$ consisting of L filter responses to a set of Gabor filters with an incremental orientation step of π/L to characterize the local pattern around the feature point $p_i(x_i, y_i)$. The principal scale $s^d_{p_i}$ and the principal orientation $\theta^d_{p_i}$ are iteratively tuned to a high accuracy. The mathematical form of a Gabor-based feature point is given as

$$\vec{V}_{p_i} = [R^{(s^d_{p_i}, \theta^d_{p_i})}(x_i, y_i), R^{(s^d_{p_i}, \theta^d_{p_i} + \frac{1}{L}\pi)}(x_i, y_i), \ldots R^{(s^d_{p_i}, \theta^d_{p_i} + \frac{L-1}{L}\pi)}(x_i, y_i)]^T$$

The similarity $S(\vec{V}_{p_i}, \vec{V}_{q_j})$ between feature points $\vec{V}_{p_i}$ and $\vec{V}_{q_j}$ can be measured by the normalized cross correlation:

$$S(\vec{V}_{p_i}, \vec{V}_{q_j}) = \frac{\vec{V}_{p_i} \cdot \vec{V}_{q_j}}{\left\|\vec{V}_{p_i}\right\| \cdot \left\|\vec{V}_{q_j}\right\|}$$

3. The homography registration

3.1 The approximate image registration: an initial solution

We shall approximate a homography by an affine transformation, and, in turn, an affine transformation by a similarity one. For the time being, we assume that the images are free from noise and missing object part.

3.2 The affine transformation matrix determination

Under an affine transformation with anisotropic scaling factor $(0 < s_1 < s_2)$, we observe that some of the Gabor-based feature points invariant under the similarity transformation remain almost invariant due to the negligible energy change when their principal orientations are nearly perpendicular to the direction of the smaller scaling s_1.

To estimate the matrix of the affine transformation, we can use merely two point pairs plus their accompanied principal orientations to replace the conventional set of three point pairs. The merit of using only two point pairs is to reduce the combinational complexity from C^n_3 to C^n_2, where n is the total number of feature points.

$$\vec{X}'_i = \begin{bmatrix} x'_i \\ y'_i \\ 1 \end{bmatrix} = \begin{bmatrix} s_1\cos\theta & -s_1\sin\theta & t_x \\ s_2\sin\theta & s_2\cos\theta & t_y \\ 0 & 0 & 1 \end{bmatrix} \begin{bmatrix} x_i \\ y_i \\ 1 \end{bmatrix} = \begin{bmatrix} a_{11} & a_{12} & a_{13} \\ a_{21} & a_{22} & a_{23} \\ 0 & 0 & 1 \end{bmatrix} \begin{bmatrix} x_i \\ y_i \\ 1 \end{bmatrix} = A\vec{X}_i$$

In Figs. 1(a) and 1(b), the unit vectors $\vec{e}_k, \vec{e}_l, \vec{e}'_k, \vec{e}'_l$ are the principal orientations of point $\vec{p}_k, \vec{p}_l, \vec{p}'_k, \vec{p}'_l$, respectively. Under the affine transformation the relationship between the two corresponding principal orientations, $(\vec{e}_k, \vec{e}'_k)$ or $(\vec{e}_l, \vec{e}'_l)$, can be shown to be

$$\left|\overrightarrow{p'_k p'_i}\right| \vec{e}'_k = A \left|\overrightarrow{p_k p_i}\right| \vec{e}_k$$

In a matrix notation,

$$\frac{\left|\overrightarrow{p'_k p'_i}\right|}{\left|\overrightarrow{p_k p_i}\right|} \begin{bmatrix} x'_{\vec{e}'_k} \\ y'_{\vec{e}'_k} \\ 0 \end{bmatrix} = \begin{bmatrix} a_{11} & a_{12} & a_{13} \\ a_{21} & a_{22} & a_{23} \\ 0 & 0 & 1 \end{bmatrix} \begin{bmatrix} x_{\vec{e}_k} \\ y_{\vec{e}_k} \\ 0 \end{bmatrix}$$

Let $s_k = \left|\overrightarrow{p'_k p'_i}\right| / \left|\overrightarrow{p_k p_i}\right|$ which is unknown.

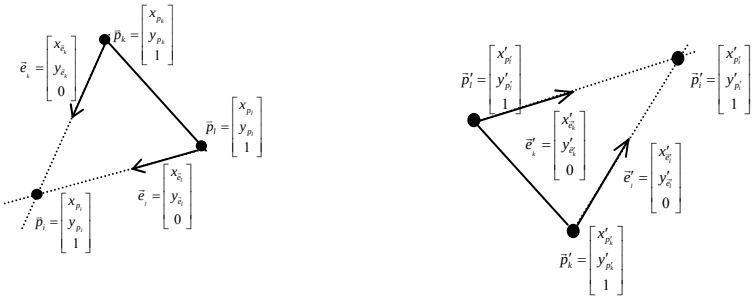

(a) **(b)**

Fig.1. **(a)** The point set $(\vec{p}_k, \vec{p}_l)$ and their individual principal orientation set $(\vec{e}_k, \vec{e}_l)$ in the reference image. **(b)** The two corresponding point set $(\vec{p}'_k, \vec{p}'_l)$ and their individual principal orientation set

Then, we have the following system of linear equations for estimating the affine transformation matrix *A*.

$$\begin{bmatrix} x_{p_k} & y_{p_k} & 1 & 0 & 0 & 0 & 0 & 0 \\ 0 & 0 & 0 & x_{p_k} & y_{p_k} & 1 & 0 & 0 \\ x_{p_l} & y_{p_l} & 1 & 0 & 0 & 0 & 0 & 0 \\ 0 & 0 & 0 & x_{p_l} & y_{p_l} & 1 & 0 & 0 \\ x_{\vec{e}_k} & y_{\vec{e}_k} & 0 & 0 & 0 & 0 & -x'_{\vec{e}'_k} & 0 \\ 0 & 0 & 0 & x_{\vec{e}_k} & x_{\vec{e}_k} & 0 & -x'_{\vec{e}'_k} & 0 \\ x_{\vec{e}_l} & y_{\vec{e}_l} & 0 & 0 & 0 & 0 & 0 & -x'_{\vec{e}'_l} \\ 0 & 0 & 0 & x_{\vec{e}_l} & y_{\vec{e}_l} & 0 & 0 & -y'_{\vec{e}'_l} \end{bmatrix} \begin{bmatrix} a_{11} \\ a_{12} \\ a_{13} \\ a_{21} \\ a_{22} \\ a_{23} \\ s_k \\ s_l \end{bmatrix} = \begin{bmatrix} x'_{p'_k} \\ y'_{p'_k} \\ x'_{p'_l} \\ y'_{p'_l} \\ 0 \\ 0 \\ 0 \\ 0 \end{bmatrix}$$

Denote the estimated matrix *A* by $T^{(0)}$ that will be used as an initial solution for computing the homography transformation in the next section. For the existence of the solution matrix $T^{(0)}$, the principal orientations $(\vec{e}_k, \vec{e}_l)$ must intersect, so do $(\vec{e}'_k, \vec{e}'_l)$. We shall discuss how to choose these appropriate orientations from the feature point set of the reference image.

3.3 Final registration

Finally, we extend the estimation from the affine transformation to a homography transformation.

$$\vec{X}' = \begin{bmatrix} x' \\ y' \\ 1 \end{bmatrix} = \begin{bmatrix} m_{11} & m_{12} & m_{13} \\ m_{21} & m_{22} & m_{23} \\ m_{31} & m_{32} & 1 \end{bmatrix} \begin{bmatrix} x \\ y \\ 1 \end{bmatrix} = M\vec{X}$$

A homography transformation differs from an affine transformation in the nonzero values of m_{31} and m_{32}. The scaling factors s_1 and s_2 vary with the point location in the image. Since the Gabor-based feature point is determined by the local (not the global) geometric structure around the feature point, so the Gabor-based feature points are invariant to the smoothly changing scaling factors.

We use the approximate transformation $T^{(0)}$ as an initial solution for applying an iterative closest point matching (ICPM) algorithm to refine the initial estimation.

Let $P = \{p_1, p_2, \cdots, p_{N_p}\}$ be a set of N_p

points in the reference image and $P' = \{p'_1, p'_2, \cdots, p'_{N_{p'}}\}$ be a set of $N_{p'}$ points in the sensed image. The ICPM algorithm iteratively transforms the sensed feature point $p'_i \in P'$ back to the reference image space and seeks for a closest point $p_i \in P$ in a predefined neighborhood such that (p'_i, p_i) is a matched point pair based on the correlation similarity measure. All the matched point psirs comprise the *corresponding point set (CPS)* and those unmatched are viewed as the outliers. Then, a new transformation $T^{(k)}$ is computed using the $CPS^{(k)}$, where *k* is iterative number (note that $CPS^{(0)}$ = *{the two starting point pairs* $(q_k, p_k), (q_l, p_l)$ *}*). The process will be repeated until no new point pair is found. We use the size of the final $CPS^{(f)}$ as a stopping criterion. The algorithm is described as follows:

Algorithm ICPM (Iterative Closest Point Matching)

Input:

1. *Two feature point sets* $P' = \{p'_1, p'_2, \cdots, p'_{N_q}\}$ *and* $P = \{p_1, p_2, \cdots, p_{N_p}\}$ *in the form of feature vectors.*
2. *The initial estimate of the transformation* $T^{(0)}$.

Output:

1. *The corresponding point set* $CPS^{(f)}$
2. *The final transformation matrix* $T^{(f)}$

Initialization:

$k = 1$

$CPS_0 = \{(p'_k, p_k), (p'_l, p_l)\}$; $d_0 = 20$

Begin

Repeat until $CPS^{(k)} \cup CPS^{(k-1)} = CPS^{(k-1)}$

1. *Construct the corresponding points set*

   $CPS^{(k)} = \cup_{i=1}^{N_{p'}} (p'_i, CC(T^{(k-1)}(p'_i), P)$

   where $CC(T^{(k-1)}(p'_i), P) = p_i$

   if the following conditions are satisfied:

   (a) Distance constraint

   $\left|T^{(k-1)}(p'_i) - p_i\right| \le d_k$

   where

   $\left|T^{(k-1)}(p'_i) - p_i\right| = \min_{p_i} \left|T^{(k-1)}(p'_i) - p_i\right|$

   $d_k = d_0 / 2^k$

   (b) Similarity constraint

   $S(p'_i, p_i) > Threshold$

   where $S(\vec{V}_{p'_i}, \vec{V}_{p_i}) = \dfrac{\vec{V}_{p'_i} \cdot \vec{V}_{p_i}}{\left\|\vec{V}_{p'_i}\right\| \cdot \left\|\vec{V}_{p_i}\right\|}$

2. *Compute the new transformation matrix* $T^{(k)}$ *using all points in the* $CPS^{(k)}$*, Update* $k = k + 1$.

End

$T^{(f)} = T^{(k)}$; $CPS^{(f)} = CPS^{(k)}$

End

4. Experiments

Computer experiments using synthetic and real image data were conducted to validate our method. All the experiments were executed on a PC, running under the Windows XP operating system and featured with an AMD K-7 1.2G Hz CPU and 512 MB RAM.

Experiment 1 for the image registration under the homography transformation

Figs. 3(a) show a reference aerial image of size 500 by 500, which is

superimposed by the extracted Gabor-based feature points. The feature points are labeled with identification numbers and attached with arrows to indicate their principal orientations. Moreover, the numbers in the parentheses indicate their principal scales. The total number of the feature points is 22 points. A synthetic image with severe perspective deformation is generated to be the sensed images, as shown in Figs. 3(b).

The first selected starting point pair happens to result in a good approximate transformation $T^{(0)}$. The result is shown in the first row of Table 1. Then, the iterative algorithm ICPM refined the approximate transformation and terminated within two iterations, producing sixteen corresponding point pairs (CPS) and a small root mean square distance error of 0.75 pixels. Table 1 also gives the two transformation matrices $T^{(i)}$ obtained at the two iterations i = 1 and 2. Fig. 4 shows the convergence of the feature points and the boundaries of the reference image under the three spatial transformations $T^{(0)}$, $T^{(1)}$ and $T^{(2)}$, respectively. The good overlapping between the two images implies that the homography estimation is correct.

Experiment 2 on image noise resistance

To demonstrate the usefulness of the strategies 2 and 3 in combating with image noise, we generate 100 noisy images by adding Gaussian noise to the reference image in Fig. 3(a), each with three different noise levels such that the signal-to-noise ratios are 9.7, 6.2 and 4.7 db, respectively.

First, we compute the principal orientations of the feature points for the 100 noisy images. In Fig. 5(a) the horizontal axis shows the ranking of the feature points according to the stability of the principal orientation $O(p_i)$, and the vertical axis shows the standard deviations of the principal orientations over the 100 noisy versions. The result reflects that the points with higher stability value of the principal orientation $O(p_i)$ will result in small variation of principal orientation under the noise effect. Meanwhile, this ranking leads to the more stable triangles used to compute the approximate transformation in the noisy images. Next, we examine the energy change of the feature points under the noise effect. The solid line in Fig. 5(b) shows the energy value of the noiseless reference feature points, and the two short horizontal lines show the energy variation range of the feature points under the noise effect with a signal-to-noise ratio 6.2 dB. The result indicates that the feature points with higher energy remain strong with the addition of noise. Thus, they should be used in the image registration. Finally, we examine the points according to the index product of $E(p_k)$ and $O(p_k)$. The result is shown in Fig. 5(c) whose annotation is same as Fig. 5(b). The result indicates that the points with larger index product have smaller

variation

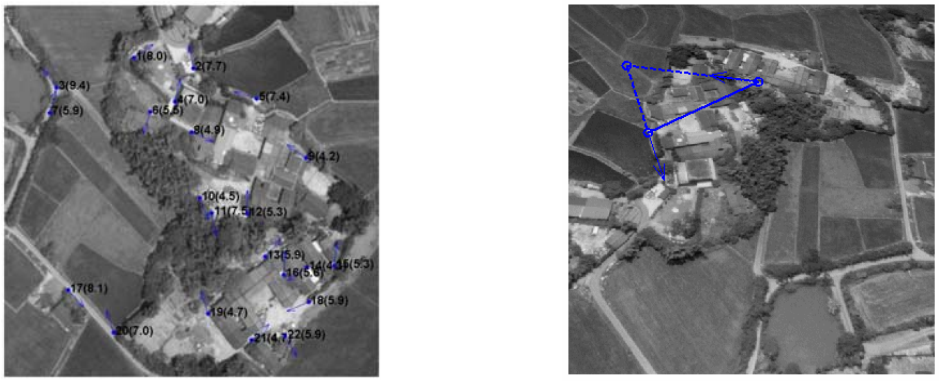

(a) (b)

Fig. 3. (a) The reference image. (b) The synthetic sensed image.

Table 1: The transformation parameters in three iterations

	$M_{3\times3}$								
	m_{11}	m_{12}	m_{13}	m_{21}	m_{22}	m_{23}	m_{31}	m_{32}	m_{33}
$T^{(0)}$	-0.6110	-1.4876	664.0500	1.0264	-0.8557	161.9824	0	0	1
$T^{(1)}$	-0.7977	-0.9341	674.8476	1.0080	-0.7286	173.6283	-0.0005	0.0018	1
$T^{(2)}$	-0.7995	-0.9120	682.9316	1.0400	-0.7318	175.3778	-0.0005	0.0020	1

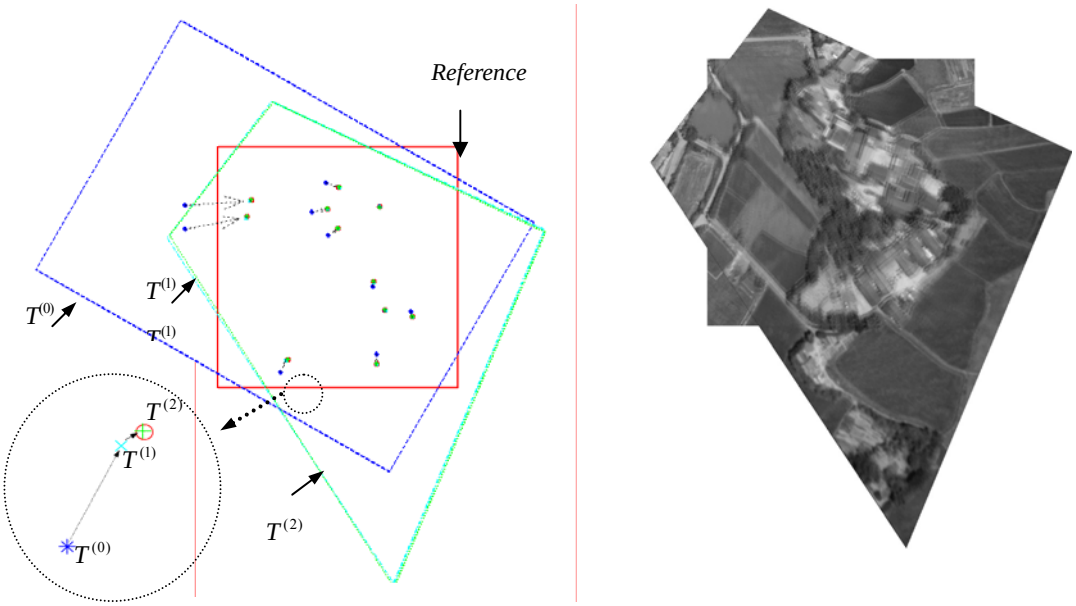

(a) (c)

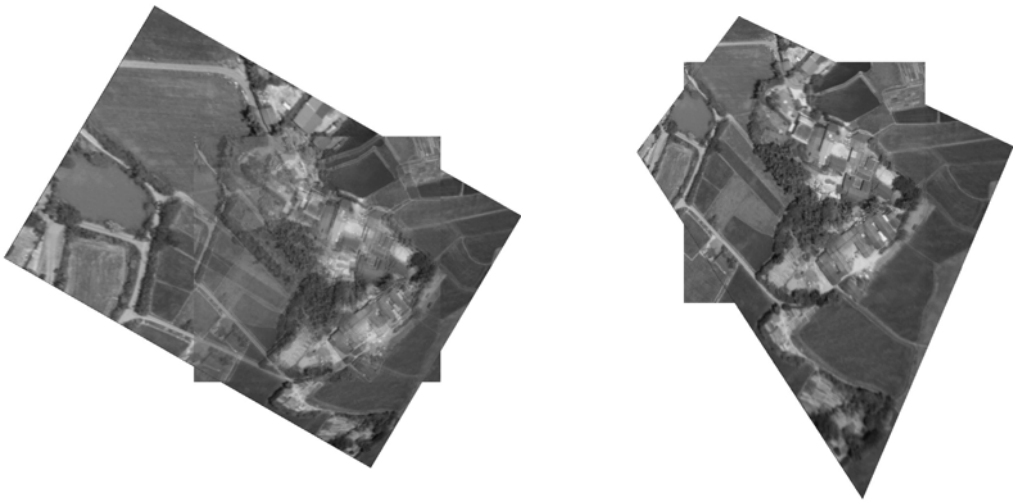

(b) (d)

Fig. 4. (a) The overlapping between the boundaries of the reference and transformed sensed images. (b)-(d) The image registration result using $T^{(0)}, T^{(1)}, T^{(2)}$, respectively.

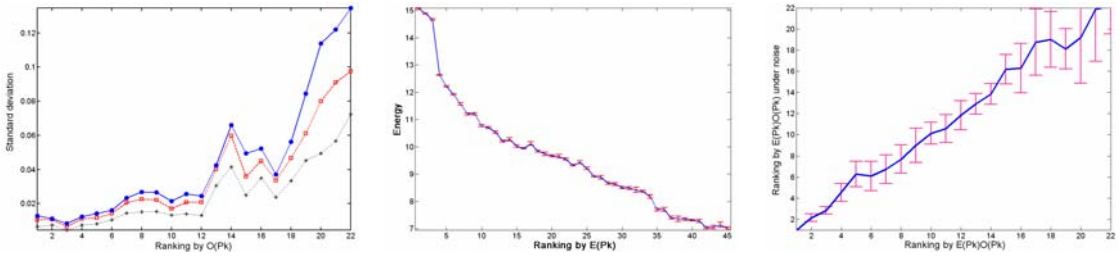

(a) (b) (c)

Fig. 5. The variations under the noise effect for (a) principal orientation, (b) energy, (c) product of principal orientation and energy.

5. Conclusion

We have applied the multi-scale, multi-orientation Gabor filtering technique to extract the robust feature points against the viewing change. Then we use the affine transformation matrix to get an initial estimation of the image registration model and refine the model by iteratively plugging the result obtained so far into an updated homorgraphy estimation. Experimental results show the registration accuracy and noise robustness of the proposed method.

Reference

[1] L. Lee, R. Romano, and G. Stein, "Monitoring Activities from Multiple Video streams: Establishing a Common Coordinate Frame," *IEEE Trans. Pattern Analysis and Machine Intelligence*, vol. 22, no. 8, pp. 758-767, Aug. 2000.

[2] Q. Zheng and R. Chellappa, ''Automatic feature

point extraction and tracking in image sequences for arbitrary camera motion,'' *I. J. Computer Vision,* vol. 15, pp. 31–76, 1995.

[3] J. Ton and A. K. Jain, "Registering Landsat Images by Point Matching", *IEEE Trans. Geosciences and Remote sensing*, Vol.27, No.5, pp.642-651, Sep. 1989.

[4] D. Shen, W. Wong, and H. H. S. Ip, "Affine-invariant image retrieval by correspondence matching of shapes", *Image and Vision Computing, vol.* **17**, pp. 489–499, 1999.

[5] G. C. Stockman, S. Kopstein, and S. Benett, " Matching images to models for registration and object detection via clustering", *IEEE Trans. Pattern Analysis and Machine Intelligence*, vol. 4, no. 3, pp. 229-241, 1982.

[6] C. Shekhar, V. Govindu, and R. Chellappa, "Multi-sensor image registration by feature consensus", *Pattern Recognition, vol.* **32**, pp. 39–52, 1999.

[7] B.D. Lucas and T. Kanade, "An Iterative Image Registration Technique with an Application to Stereo Vision," *Proc. Image Understanding Workshop*, pp. 121-130, 1981.

[8] Y. Caspi, M. Irani, "Spatio-Temporal Alignment of Sequences", IEEE *Tran. PAMI*, vol. 24, no. 11, 2002.

[9] L. G. Brown, "A survey of image registration techniques", *ACM Computing Surveys*, vol. 24, no. 4, pp. 335-376, Dec. 1992.

[10] J. B. A. Maintz _ and M. A. Viergever, "A survey of medical image registration" medcal image analysis, vol. 2, no. 1, pp. 1–37, 1998.

[11] T. Mäkelä, P. Clarysse, O. Sipilä, N. Pauna, Q. C. Pham, T. Katila, and I. E. Magnin, "A Review of Cardiac Image Registration Methods" *IEEE Tran. Medical Imaging*, vol. 21, no. 9, 2002.

[12] Q. M. Tieng, W. W. Boles, "Wavelet-based affine invariant representation: a tool for recognizing planar objects in 3D space", *IEEE Trans. Pattern Analysis and Machine Intelligence*, vol. 19, no. 8, pp. 846-857, Aug. 1997.

[13] Z. Yang and F. S. Cohen, "Image Registration and Object Recognition Using Affine Invariants and Convex Hulls", *IEEE Trans. Image Processing*, vol. 8, no.7, pp. 934-946, July 1999.

[14] O. Faugeras, "Three Dimensional Computer Vision: A Geometric Viewpoint", *MIT Press*, 1993.

[15] Z. Zhang, R. Deriche, O. Faugeras, Q. T. Luong, "A robust technique for matching two uncalibrated images through the recovery of the unknown epiploar geometry ", *Artificial Intelligence*, vol. 78, pp. 87-119, 1995.

[16] L.M.G. Fonseca and M.H.M. Costa, "Automatic registration of satellite images", Proceedings of Brazilian Symposium on *Computer Graphics and Image Processing* X , pp. 219 –226,1997.

[17] J. Zhou and J. Shi, "A robust algorithm for feature point matching", *Computers & Graphics*, vol. 26, pp. 429-436, 2002.

[18] P. Bao and D. Xu, "Complex wavelet-based image mosaics using edge-preserving visual perception modeling", *Computer & Graphics*, vol. 23, pp. 309-321, 1999.

[19] J. W. Hsieh, H. Y. Liao, K. C. Fan, M. T. Ko and Y. P. Hung, "Image Registration Using a New Edge-based Approach", *Computer Vision and Image Understanding*, vol. 67, no. 2 pp. 112-130, Aug. 1997.

[20] Q. Zheng and R. Chellappa, "A computational vision approach to image registration", *IEEE Tran. Image Processing*, vol. 2, no. 3, pp. 311 -326, 1993.

[21] J. M. Chiu, Z. Chen, J. H. Chuang and T. L. Chia (1997), "Determination of feature

correspondences in stereo images using a calibration polygon," Pattern Recognition, vol. 10, no.9, pp. 1387-1400.

[22] G. Lei, "Recognition of planar objects in 3-D space from single perspective views using cross ratio," IEEE Trans. Robotics and Automation, Vol. 8, No. 4, pp. 432-437, 1990.

[23] Y. Liu and M. A Rodrigues, "Eliminating false matches in image registration through geometric histograms from reflected correspondence vectors", *Proc. IEEE Conf. Intelligent Robots and Systems*, pp. 1997-2002, 2001.

[24] P. Werth and S. Scherer, "Robust subpixel stereo matching by relaxation of match candidates", *Proc. Fist Int'l workshop on image and signal processing and analysis*, pp. 14-15, 2000.

[25] F. Ola and J. A. Marchant, "Matching feature points in image sequences through a region-based method", *Computer Vision and Image Understanding*, vol. 66, no. 3, pp. 271-285, 1997.

[26] H. Lamdan, J. T. Schwartz and H. J. Wolfson, "Affine invariant model-based object recognition", *IEEE Trans. Robotics and Automation*, vol. 6, no. 5, pp. 578-589, Oct. 1990.

[27] T. Suk and J. Flusser, "Point-based projective invariants", *Pattern Recognition*, vol. 33 pp. 251-261, 2000.

[28] S. Irani , P. Raghavan, "Combinatorial and experimental results for randomized point matching algorithms", *Computational Geometry* , vol. 12 , pp. 17–31, 1999.

[29] S. H. Chang, F. H. Cheng W. H. Hsu and G. Z. Wu, "Fast Algorithm for Point Pattern Matching: Invariant to Translation, Rotation and Scale Changes", *Pattern Recognition*, vol.30, no.2, pp.311-320, 1997.

[30] F. H. Cheng, "Point pattern matching algorithm invariant to geometrical transformation and distortion". *Pattern Recognition Letter*, vol.17 pp.1429-1435, 1996.

[31] D. M. Mount, N. S. Netanyahu and J. L. Moigne, "Efficient algorithm for robust feature matching", *Pattern Recognition*, vol.32, pp.17-38, 1999.

[32] J. Flusser, "A moment-based approach to registration of images with affine geometric distortion", *IEEE Trans. Geoscience and Remote Sensing,* vol. 32, no. 2, pp. 382-387, 1994.

[33] E. De Castro and C. Morandi, ''Registration of translated and rotated image using finite Fourier transform,'' *IEEE Trans. Pattern Analysis and Machine Intelligence,* vol. 9, no. 5, pp. 700–703, Sept. 1987.

[34] B. S. Reddy and B. N. Chatterji, "An FFT-based technique for translation, rotation and scale-invariant image registration", vol. 5, no. 8, pp. 1266-,1271, 1996.

[35] S. K. Sun, Z Chen and T. L. Chia, "Invariant feature extraction and object shape matching using Gabor filtering", *Lecture notes in computer science, Springer*, vol. 2314, pp. 95-104, 2002.

[36] Y. Ohta and T. Kanade, "Stero by intra- and inter-scanline search," IEEE TPAMI, 7(2), pp. 139-154, 1985.

[37] S. Christy and R. Horaud, "Euclidean shape and motion from multiple perspective views by affine iterations". IEEE TPAMI, Vol 18, N0, 11, pp. 1098-1104,1996.

[38] H. Aanas, R. Fisker, and K. Astrom, "Robust factorization," IEEE TPAMI, Vol. 24, No. 9, pp. 1215 -1225, 2002.

[39] J.P. Costerira and T. Kanade, "A multibody factorization method for independently moving objects," IJCV, 29(3), pp. 159-179, 1998.

[40] R.C. Bolles and M.A. Fischler, " A RANSAC-based approach to model fitting and its application to finding cylinders in

range data," Proc. International Joint Conf. on Artificial Intelligence, 1981.